PROBLEMS IN NONLINEAR ACOUSTICS:

SURFACE ACOUSTIC WAVES, DIFFRACTING SOUND BEAMS, AND FLUID-SOLID INTERFACE EFFECTS

Mark F. Hamilton

DEPARTMENT OF MECHANICAL ENGINEERING
THE UNIVERSITY OF TEXAS AT AUSTIN
AUSTIN, TEXAS 78712-1063

31 May 1994

Sixth Annual Summary Report
ONR Grants N00014-89-J-1003 (primary grant)
and N00014-93-1-1135 (AASERT)

Prepared for:

OFFICE OF NAVAL RESEARCH
800 NORTH QUINCY STREET
ARLINGTON, VA 22217-5660

REPORT DOCUMENTATION PAGE

Form Approved
OMB No. 0704-0188

1. AGENCY USE ONLY (Leave blank)	2. REPORT DATE	3. REPORT TYPE AND DATES COVERED
	31 May 1994	Summary: 01 Sep 93 - 31 May 94

4. TITLE AND SUBTITLE
PROBLEMS IN NONLINEAR ACOUSTICS: Surface Acoustic Waves, Diffracting Sound Beams, and Fluid-Solid Interface Effects

5. FUNDING NUMBERS
PE 61153N
G N00014-89-J-1003
(and G N00014-93-1-1135)
TA 3126943

6. AUTHOR(S)
Mark F. Hamilton

7. PERFORMING ORGANIZATION NAME(S) AND ADDRESS(ES)
Department of Mechanical Engineering
The University of Texas at Austin
Austin, TX 78712-1063

8. PERFORMING ORGANIZATION REPORT NUMBER
ASR-6

9. SPONSORING/MONITORING AGENCY NAME(S) AND ADDRESS(ES)
Office of Naval Research
ONR 331
800 North Quincy Street
Arlington, VA 22217-5660

10. SPONSORING/MONITORING AGENCY REPORT NUMBER

11. SUPPLEMENTARY NOTES

12a. DISTRIBUTION/AVAILABILITY STATEMENT
Approved for public release;
Distribution unlimited.

12b. DISTRIBUTION CODE

13. ABSTRACT *(Maximum 200 words)*

Three subject areas, with emphasis on nonlinear acoustics, are discussed in this annual summary report: (1) Surface Acoustic Waves [evolution equations, generalized model equations for complex space-time dependencies, and nonlinearity coefficients for Rayleigh waves, and model equation for Stoneley waves]; (2) Diffracting Sound Beams [modeling of noise and relaxation, measurements of focused beams, and transient solution for radiation from a parabolic antenna]; and (3) Fluid-Solid Interface Effects [comparisons of 2-D and 3-D reflection for piston and Gaussian sources].

14. SUBJECT TERMS
nonlinear acoustics, Rayleigh waves, Stoneley waves, sound beams, pulses, noise, nondestructive evaluation

15. NUMBER OF PAGES
27

16. PRICE CODE

17. SECURITY CLASSIFICATION OF REPORT	18. SECURITY CLASSIFICATION OF THIS PAGE	19. SECURITY CLASSIFICATION OF ABSTRACT	20. LIMITATION OF ABSTRACT
UNCLASSIFIED	UNCLASSIFIED	UNCLASSIFIED	

CONTENTS

INTRODUCTION

This annual summary report describes research performed from 1 September 1993 through 31 May 1994 with financial support from ONR Grant N00014-89-J-1003 (with the exception of Landsberger's work, which is supported by ONR Grant N00014-93-1-1135; see Sec. III). Three main subject areas are discussed in this report, with emphasis on nonlinear effects:

I. Surface Acoustic Waves

II. Diffracting Sound Beams

III. Fluid-Solid Interface Effects

Contributions to these projects were made by the following individuals:

Senior Personnel

- M. F. Hamilton, principal investigator
- Yu. A. Il'insky, visiting scientist
- E. A. Zabolotskaya, visiting scientist

Graduate Students

- M. A. Averkiou, Ph.D. student in Mechanical Engineering
- E. Yu. Knight, M.A. student in Physics
- B. J. Landsberger, Ph.D. student in Mechanical Engineering
- Y.-S. Lee, Ph.D. student in Mechanical Engineering
- G. D. Meegan, Ph.D. student in Physics

Professor Il'insky, on leave from the Department of Physics at Moscow State University, performed research in our group for three of the nine months covered by this report (September and October of 1993, and January of 1994). Dr. Zabolotskaya is on leave from the General Physics Institute in Moscow.

The main source of financial support, in addition to that provided by ONR, has been the David and Lucile Packard Foundation Fellowship for Science and Engineering. Computing resources were provided by The University of Texas System Center for High Performance Computing.

The following manuscripts, abstracts, and dissertations, which contain work supported at least in part by ONR, have been published (or submitted for publication) since 1 September 1993.

Refereed Journals

- M. A. Averkiou, Y.–S. Lee, and M. F. Hamilton, "Self-demodulation of amplitude and frequency modulated pulses in a thermoviscous fluid," *J. Acoust. Soc. Am.* **94**, 2876–2883 (1993).
- M. F. Hamilton, Yu. A. Il'insky, and E. A. Zabolotskaya, "Nonlinearity in Rayleigh waves," submitted to *J. Acoust. Soc. Am.* in October 1993.
- D. J. Shull, E. E. Kim, M. F. Hamilton, and E. A. Zabolotskaya, "Diffraction effects in nonlinear Rayleigh wave beams," submitted to *J. Acoust. Soc. Am.* in December 1993.
- M. F. Hamilton, Yu. A. Il'insky, and E. A. Zabolotskaya, "Evolution equations for nonlinear Rayleigh waves," submitted to *J. Acoust. Soc. Am.* in February 1994.
- Y.–S. Lee and M. F. Hamilton, "Time domain modeling of pulsed finite amplitude sound beams," submitted to *J. Acoust. Soc. Am.* in March 1994.

Oral Presentation Abstracts

- M. A. Averkiou, I. R. S. Makin, and M. F. Hamilton, "Measurements of focused, finite amplitude sound beams reflected from curved targets," *J. Acoust. Soc. Am.* **94**, 1876 (1993).
- M. A. Averkiou and M. F. Hamilton, "Measurements of finite amplitude pulses radiated by plane circular pistons in water," *J. Acoust. Soc. Am.* **94**, 1876 (1993).
- D. J. Shull, E. E. Kim, M. F. Hamilton, and E. A. Zabolotskaya, "Diffracting nonlinear Rayleigh wave beams," *J. Acoust. Soc. Am.* **95**, 2864 (1994).

Dissertations

- Y.–S. Lee, "Numerical solution of the KZK equation for pulsed finite amplitude sound beams in thermoviscous fluids," Ph.D. Dissertation, The University of Texas at Austin (December 1993). Lee is currently employed by an automobile manufacturer in South Korea.
- M. A. Averkiou, "Experimental investigation of propagation and reflection phenomena in finite amplitude sound beams," Ph.D. Dissertation, The University of Texas at Austin (May 1994). Averkiou is currently employed by Applied Physics Laboratory, University of Washington, Seattle, Washington.

I. Surface Acoustic Waves

Portions of the work described in this section were performed by Yu. A. Il'insky, E. Yu. Knight, G. D. Meegan, and E. A. Zabolotskaya. Four related investigations are described below, all originating from Zabolotskaya's theoretical framework:[1] differential time-domain evolution equations for nonlinear Rayleigh waves, model equations which account for arbitrary time and space depencencies in nonlinear Rayleigh waves, definition and comparison of nonlinearity coefficients associated with Rayleigh waves, and nonlinear Stoneley waves.

A. Evolution Equations for Nonlinear Rayleigh Waves

This project is completed, and the following discussion is based on two articles[2, 3] currently in review for publication in *Journal of the Acoustical Society of America.*

Evolution equations in the time domain were derived for nonlinear Rayleigh waves on the surface of an isotropic solid. Two evolution equations were derived, one in terms of the real horizontal displacement component, and the other in terms of a complex displacement variable. The motivation to derive time domain evolution equations for nonlinear Rayleigh waves is the wealth of experience acquired from the many time domain studies of finite amplitude sound in fluids, e.g., based on the Burgers equation[4] (for plane waves) and the KZK equation[5] (for diffracting beams). Time domain equations for Rayleigh waves should thus permit greater understanding of the similarities and differences with nonlinear effects in fluids.

The evolution equations are derived from the theoretical model developed by Zabolotskaya.[1] To simplify the analysis, not all nonlinear terms are included. However, the terms that are retained have been shown[2, 3] to account qualitatively for all nonlinear effects predicted by the complete theoretical model. Moreover, the present analysis can be extended to include the remaining nonlinear terms. We note that differential evolution equations for nonlinear Rayleigh waves, derived from the fundamental equations of motion, have not appeared previously in the literature.

The analysis begins with the coupled spectral equations derived by Zabolotskaya[1] for plane waves:

$$\frac{dV_n}{dX} = -n^2 \sum_{l+m=n} \frac{|ml|}{ml} R_{ml} V_m V_l - n^2 A V_n \,, \tag{1}$$

where V_n are dimensionless spectral components in a Fourier series expansion of the horizontal and vertical velocity components, X is distance along the surface of the solid, R_{ml} is the nonlinearity matrix that depends on the frequencies of the interaction components, and A is an absorption coefficient. The nonlinearity matrix has the form

$$R_{ml} = \frac{\alpha}{|l+m|\xi_l + |l|\xi_t + |m|\xi_t} + \frac{\alpha}{|l+m|\xi_t + |l|\xi_t + |m|\xi_l} + \frac{\alpha}{|l+m|\xi_t + |l|\xi_l + |m|\xi_t}$$

$$+\frac{\beta}{|l+m|\xi_t+|l|\xi_l+|m|\xi_l}+\frac{\beta}{|l+m|\xi_l+|l|\xi_t+|m|\xi_l}+\frac{\beta}{|l+m|\xi_l+|l|\xi_l+|m|\xi_t}$$
$$+\frac{3\gamma}{|l+m|\xi_l+|l|\xi_l+|m|\xi_l}, \tag{2}$$

where the coefficients α, β, and γ depend on both the second and third order constants for an isotropic elastic solid (ξ_l and ξ_t depend only on the second order constants). We have shown[2] that the "α terms," the "β terms," and the "γ term" in the matrix R_{ml} produce very similar nonlinear effects. Because of the complexity involved in the derivation of an evolution equation, we therefore concentrate on the effect due to only one of these terms. For simplicity we choose the γ term. Setting $\alpha = \beta = 0$, we have transformed Eq. (1) into the time domain and thus derived two alternative evolution equations in terms of particle displacement variables.

The first evolution equation is expressed in terms of the complex particle displacement variable D at the surface of the solid:

$$\frac{\partial D}{\partial X}=\frac{1}{2}\left(\frac{\partial D}{\partial \theta}\right)^2+\frac{1}{2}(1+i\mathcal{H})\left[D\frac{\partial^2 D^*}{\partial\theta^2}+\frac{\partial D}{\partial\theta}\frac{\partial D^*}{\partial\theta}\right]+A\frac{\partial^2 D}{\partial\theta^2}, \tag{3}$$

where θ is dimensionless retarded time, and $\mathcal{H}$ is the Hilbert transform operator defined by the principal value of the integral

$$\mathcal{H}[f]=\frac{1}{\pi}\int_{-\infty}^{\infty}\frac{f(t')}{t'-t}\,dt'. \tag{4}$$

The horizontal and vertical particle velocity components at the surface, V_x and V_z, respectively, are obtained from the real and imaginary parts of D:

$$V_x=-(\eta+\xi_t)\frac{\partial}{\partial\theta}(\mathrm{Re}\,D), \tag{5}$$

$$V_z=-(1+\eta\xi_l)\frac{\partial}{\partial\theta}(\mathrm{Im}\,D), \tag{6}$$

where η depends on the second order elastic constants. Equations (1) and (3) [with $\alpha = \beta = 0$ in Eq. (2)] provide equivalent descriptions of the Rayleigh wave on the surface of the solid, and each can be solved with standard finite difference methods. Numerical solutions of the two equations are shown in Fig. 1 for a wave that is sinusoidal at the source ($X = 0$). Minor discrepancies are observed after shock formation, which are due to using only a finite number of spectral components in the numerical solution of Eq. (1), and from discretization of the time waveform in the numerical solution of Eq. (3). The solutions converge, however, with increasing numbers of frequency components and time samples used in the calculations. Comparison of the waveforms in Fig. 1 with those calculated in previous articles[1,6] [the α and β terms were retained in Eq. (2) for the calculations reported in Refs. 1 and 6]

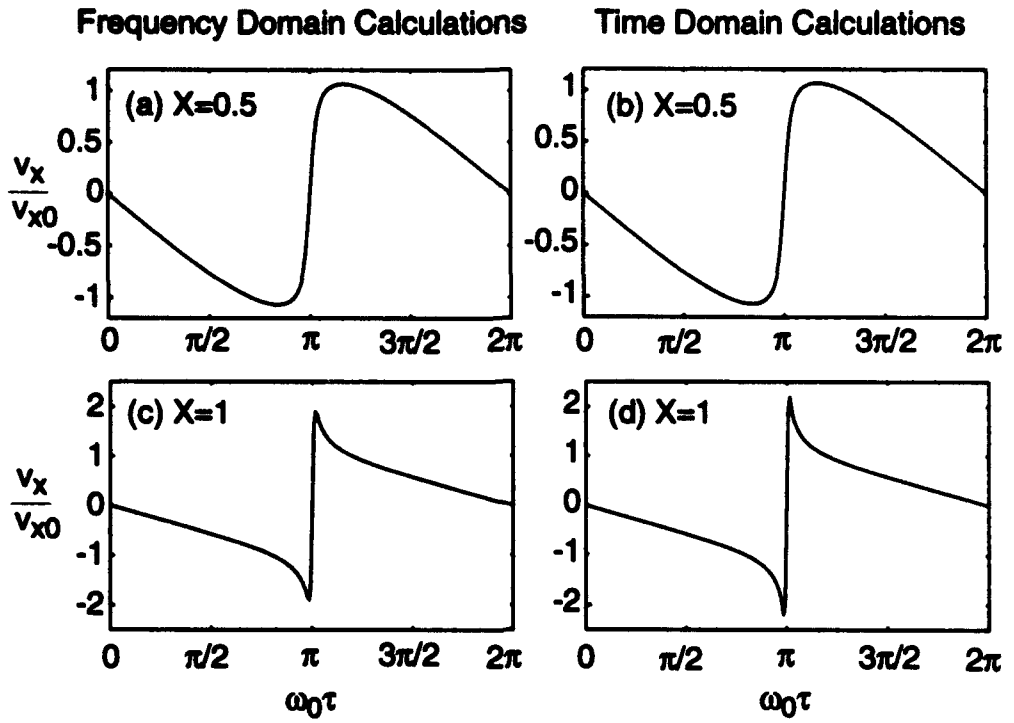

Figure 1: Comparison of horizontal velocity waveforms calculated with the frequency domain equation (left column) and with the time domain equation (right column) at two distances, $X = 0.5$ (upper row) and $X = 1$ (lower row).

reveals that the γ term alone, and therefore Eq. (3), indeed account for all main effects of nonlinearity in Rayleigh wave propagation.

An alternative version of Eq. (3) can be derived in terms of a real displacement component d:

$$\frac{\partial d}{\partial X} = \frac{1}{4}\frac{\partial^2 d^2}{\partial \theta^2} + \frac{1}{2}\mathcal{H}\left[d\,\mathcal{H}\left[\frac{\partial^2 d}{\partial \theta^2}\right]\right] + A\frac{\partial^2 d}{\partial \theta^2}\,. \tag{7}$$

The corresponding velocity components are now obtained from the relations

$$V_x = -\frac{1}{2}(\eta + \xi_t)\frac{\partial d}{\partial \theta}\,, \tag{8}$$

$$V_z = \left(\frac{1 + \eta\xi_t}{\eta + \xi_t}\right)\mathcal{H}[V_x]\,. \tag{9}$$

Methods used to solve Eq. (3) can also be applied to Eq. (7).

We conclude by noting that diffraction effects[7] are easily included in Eqs. (3) and (7), which yield KZK-type equations for nonlinear Rayleigh waves.

B. Generalized Equations for Nonlinear Rayleigh Waves

This research was performed by E. Yu. Knight, who received partial financial support from the Earth and Environmental Sciences Division at Los Alamos National Laboratory. She is scheduled to receive her M.A. in Physics in December 1994. Knight has generalized the spectral equations derived by Zabolotskaya[1] to include arbitrary spatial dependencies (e.g., not restricted to progressive plane, cylindrical, or quasiplane waves) and arbitrary time dependencies (i.e., not necessarily periodic waveforms).

We begin by presenting the equations for plane waves with arbitrary time dependencies. The horizontal and vertical velocity components in the elastic half space $z \leq 0$ are now expressed as continuous Fourier integrals, rather than discrete Fourier series, as follows:

$$v_x(x,z,t) = \int_{-\infty}^{\infty} u_x(z,\omega)\tilde{v}(x,\omega)e^{-i\omega(t-x/c_R)}\,\frac{d\omega}{2\pi}\,, \tag{10}$$

$$v_z(x,z,t) = \int_{-\infty}^{\infty} u_z(z,\omega)\tilde{v}(x,\omega)e^{-i\omega(t-x/c_R)}\,\frac{d\omega}{2\pi}\,, \tag{11}$$

where the depth dependent functions are defined as in previous work:[1, 6]

$$u_x(z,\omega) = \xi_t e^{\omega\xi_t z/c_R} + \eta e^{\omega\xi_l z/c_R}\,, \tag{12}$$

$$u_z(z,\omega) = e^{\omega\xi_t z/c_R} + \eta\xi_l e^{\omega\xi_l z/c_R}\,. \tag{13}$$

The resulting equation for the complex spectral amplitude $\tilde{v}(x,\omega)$ in Eqs. (10) and (11) becomes

$$\frac{\partial\tilde{v}(x,\omega)}{\partial x} = -\frac{\mu\omega^2}{\rho\zeta c_R^4}\int_{-\infty}^{\infty}\frac{|\omega'(\omega-\omega')|}{\omega'(\omega-\omega')} \times R(\omega',\omega-\omega')\tilde{v}(x,\omega')\tilde{v}(x,\omega-\omega')\,\frac{d\omega'}{2\pi}\,. \tag{14}$$

The function $R(\omega_1,\omega_2)$ is the same as the matrix in Eq. (2), with ω_1 and ω_2 in place of m and l. With the integrals in Eqs. (10) and (11) replaced by discrete Fourier series, Eq. (14) reduces to the set of coupled discrete equations derived by Zabolotskaya,[1] namely, Eq. (1) with $A = 0$.

We now remove the restriction to plane waves, and begin by expressing the horizontal and vertical velocity components in the form

$$\mathbf{v}(\mathbf{r},z,t) = c_R\nabla_\perp\int_{-\infty}^{\infty} u_r(z,\omega)\tilde{V}(\mathbf{r},\omega)\omega^{-1}e^{-i\omega t}\,\frac{d\omega}{2\pi}\,, \tag{15}$$

$$v_z(\mathbf{r},z,t) = \int_{-\infty}^{\infty} u_z(z,\omega)\tilde{V}(\mathbf{r},\omega)e^{-i\omega t}\,\frac{d\omega}{2\pi}\,, \tag{16}$$

where $\mathbf{v} = (v_x, v_y)$, $\mathbf{r} = (x, y)$, and $\nabla_\perp$ is the gradient in the (x, y) plane. The equation obtained for $\tilde{V}(\mathbf{r}, \omega)$ is

$$\left(\nabla_\perp^2 + \frac{\omega^2}{c_R^2}\right)\tilde{V}(\mathbf{r},\omega) = -\frac{2i\omega^3\mu}{\rho\zeta c_R^5}\int_{-\infty}^{\infty}\frac{|\omega'(\omega-\omega')|}{\omega'(\omega-\omega')} \times R(\omega', \omega-\omega')\tilde{V}(\mathbf{r},\omega')\tilde{V}(\mathbf{r},\omega-\omega')\frac{d\omega'}{2\pi}. \quad (17)$$

The model equations used previously for cylindrical Rayleigh waves[1, 6] and for diffracting Rayleigh wave beams[7] can be derived as approximations of Eq. (17). In these earlier articles,[1, 6, 7] the terms which account for cylindrical spreading and diffraction were introduced in an ad hoc manner. Equation (17) thus permits these previous results to be derived more rigorously. In addition, Eq. (17) applies to compound wave fields (e.g., standing waves) as well as progressive wave fields.

C. Nonlinearity Coefficients for Rayleigh Waves

This research was also performed by Knight. Comparison of Zabolotskaya's model equation[1] with one derived perviously by Parker[8] was performed. Also, a quantitative investigation of the shock formation distance was conducted, which led to a consistent definition for a coefficient of nonlinearity.

We first discuss comparison with the model equation for nonlinear Rayleigh waves derived by Parker,[8] who expresses his result in essentially the same form as Eq. (1). Whereas Zabolotskaya used Hamiltonian formalism to derive Eq. (1), Parker used a dynamical approach which begins with the governing nonlinear differential equations of motion and the nonlinear free surface boundary conditions (this same starting point has been used by all previous authors who investigated nonlinear Rayleigh waves, except Zabolotskaya). Parker derived an evolution equation for the Fourier transform of the vertical component of the particle displacement as a condition for ensuring that corrections to the displacement predicted by linear theory are sufficiently small everywhere. Following considerable algebraic manipulations, Knight has shown that the final equations obtained by Parker are in fact identical to those derived by Zabolotskaya, even though the derivations are fundamentally different, and the nonlinearity matrices as expressed by Parker and Zabolotskaya are considerably different in appearance.

We now consider the shock formation distance for a nonlinear Rayleigh wave. Recalling Eq. (2), we see that the "strength" of nonlinear interaction between any two given spectral components in a Rayleigh wave is a function of the frequencies of the two components. In contrast, the coefficient of nonlinearity for sound waves in fluids is independent of frequency. Consequently, whereas an analytic expression for the shock formation distance in a fluid is readily defined, the same is not true for nonlinear Rayleigh waves. Using the rate of second harmonic generation as a measure of waveform distortion, we proposed in an earlier article[6] a simple expression for

the Rayleigh wave shock formation distance. Via comparison with direct numerical solutions of Eq. (1), Knight has shown that the earlier expression[6] overestimates the shock formation distance by approximately 10–20%.

An alternative expression for the shock formation distance was derived by Knight in terms of an integral over the nonlinearity matrix $R(\omega_1, \omega_2)$. This alternative approach accounts (in an approximate way) for all spectral interactions, not just the lowest order contribution to second harmonic generation. Her expression for the shock formation distance is

$$\overline{x} = c_R^2 / \beta \omega_0 v_{x0} \,, \tag{18}$$

where ω_0 is the frequency of the source waveform, v_{x0} is the peak horizontal velocity amplitude at the source, and the coefficient of nonlinearity β is determined by the integral over $R(\omega_1, \omega_2)$. In contrast to the result proposed in Ref. 6, Eq. (18) agrees with numerically calculated shock formation distances to within 5%.

The form of Eq. (18) was chosen to be consistent with the expression for the shock formation distance of a sound wave in a fluid, and therefore β may be compared with the more familiar coefficient of nonlinearity in acoustics. In Table 1 are listed values of β calculated for materials having reasonably accurate values for the third order elastic constants reported in the literature. The first five materials listed are all homogeneous solids, and all have values of β that are of order one, as in fluids. The last five materials are rocks that contain microcracks and other inhomogeneous features, and the nonlinearity coefficients are of order 10^3.

Material	β
Polystyrene	0.84
Nickel steel 535	0.85
Steel 60 C2H2A	1.03
Armco iron	2.03
Pyrex	2.42
Barre Granite	200
Dry Marble D82	593
Water Saturated F32 Thermally Cracked	1523
Dry F32 Fountainebleau Sandstone	3201
Dry F32 Thermally Cracked	4192

Table 1: Rayleigh wave nonlinearity coefficients for various materials.

D. Nonlinear Stoneley Waves

The investigation of nonlinear Stoneley waves is being performed by G. D. Meegan, whose funding has been provided through an AASERT (Augmentation Award for Science and Engineering Training) extension of the present ONR grant. This extension began in September 1992. Meegan is scheduled to take his Ph.D. qualifying exam in Physics in fall 1994.

A Stoneley wave propagates along the interface of two elastic solids in nonslip contact. To some extent, a Stoneley wave may be thought of as a two-sided Rayleigh wave, insofar as the disturbance decays exponentially with distance away from the interface in either solid. However, the particle motion in the two solids differs. Figure 2(a) depicts the horizontal particle displacement u_x and vertical particle displacement u_z for a Stoneley wave at a glass-steel interface. In the steel, the particle trajectory resembles that for a Rayleigh wave, namely, it traces a retrograde elliptical orbit (with respect to the direction of wave propagation) at the interface, reverses direction at a depth of approximately one-third wavelength (note the sign change in the horizontal component), and decays exponentially thereafter with further increase in depth. In the glass, however, the particle motion is prograde at all depths, never changing direction of rotation. Moreover, as indicated by the shaded areas in Fig. 2(b), only material combinations with certain parameter relations can support Stoneley waves (Poisson's ratio was assumed to be $\nu = 0.25$ for each solid, and the axes specify the ratios of the densities and shear moduli of the two solids).

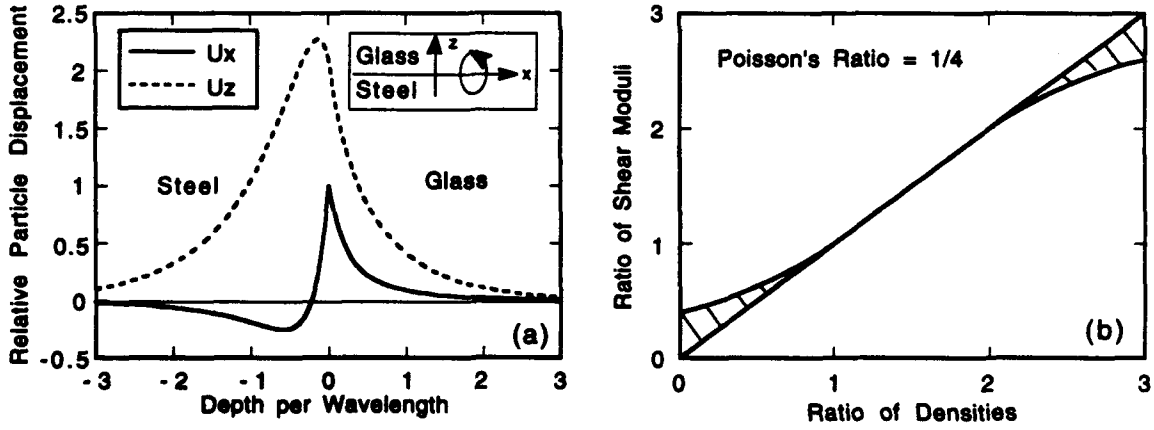

Figure 2: (a) Stoneley wave particle displacements, and (b) parameter regions for which Stoneley waves exist.

Meegan's derivation of the equation for nonlinear Stoneley waves at the interface separating two isotropic solids follows closely the method developed by Zabolotskaya[1] for nonlinear Rayleigh waves. Specifically, Hamiltonian formalism is used. One begins with Fourier expansions based on a modification of linear theory for the particle displacement in each solid. The kinetic and potential energy functions are

obtained by integrating over the two half spaces occupied by the two solids (terms through cubic order in the displacement are retained in the strain energy function). Finally, generalized displacement and momentum variables are introduced, which are interrelated through the Hamiltonian. The resulting system of equations can be solved for the complex spectral amplitudes in the Stoneley wave. The resulting set of coupled equations for the spectral amplitudes of the velocity components can be written in the form

$$\frac{dv_n}{dx} = -\frac{\mu_1 n^2 k_S}{2\rho_1 c_S^3 \zeta_S} \sum_{m+l=n} \frac{ml}{|ml|} R^S_{ml} v_m v_l \,, \tag{19}$$

where the subscript "1" indicates shear modulus (μ) or density (ρ) in medium 1. In the absence of a second medium (i.e., with a free surface bounding medium 1), replace the superscripts and subscripts S by 1, and Eq. (19) reduces to Zabolotskaya's result for Rayleigh waves. For a Stoneley wave, the nonlinearity matrix is now given by

$$R^S_{ml} = R^{(1)}_{ml} + K R^{(2)}_{ml} \,, \tag{20}$$

where $R^{(i)}_{ml}$ $(i = 1, 2)$ is given by Eq. (2) for medium i, and K depends only on the second order elastic constants for the two media. We note that the nonlinearity matrix R^S_{ml} exhibits precisely the same symmetries as the nonlinearity matrix R_{ml} for Rayleigh waves. Consequently, the theoretical description of nonlinear Stoneley waves given by Eq. (19) is amenable to the same mathematical techniques that have been employed in our recent investigations of nonlinear Rayleigh waves.

In Fig. 3 we compare propagation curves for the fundamental through third harmonic components in a Rayleigh wave in steel (dashed lines) and in glass (dotted lines), with those for a Stoneley wave that propagates along a steel-glass interface (solid lines). The waves are sinusoidal at the source, where the horizontal velocity components are equal for all three cases. Nonlinearity is seen to be stronger for the Rayleigh waves in the individual materials (i.e., more rapid harmonic generation) than for the Stoneley wave at the interace when the two materials are in contact. The difference increases slightly if the vertical velocities, rather than the horizontal velocities, are matched at the source. The decrease in nonlinearity is connected mainly with the decrease in the ratio E_3/E_2, where E_n is the integrated strain energy at order n in terms of the particle displacement. Whether nonlinearity is normally weaker in Stoneley waves than in Rayleigh waves has yet to be ascertained.

Equation (19) shall be used to investigate Stoneley waves systematically with techniques that have been established for nonlinear Rayleigh waves. Experimental work is also underway.

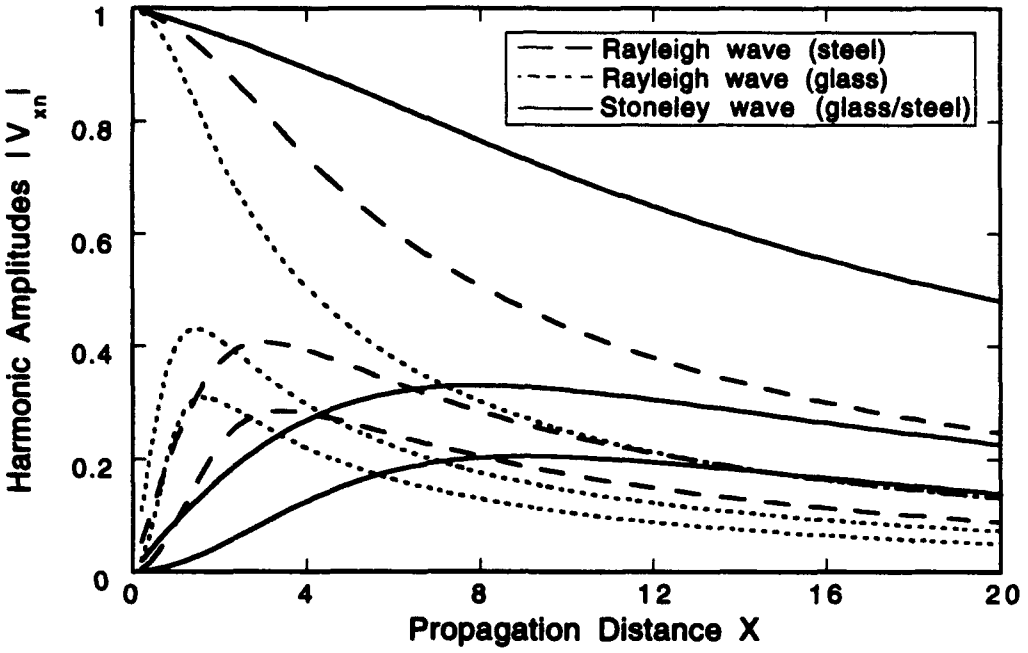

Figure 3: Fundamental, second, and third harmonic propagation curves for three types of surface waves.

II. Diffracting Sound Beams

A. Pulsed Finite Amplitude Sound Beams

The material reported in this section concludes the numerical investigation of pulsed finite amplitude sound beams by Y.–S. Lee, who received his Ph.D. in Mechanical Engineering for this work in December 1993.[9] The results reported below were obtained during the past year, and they are included in an article[10] submitted in March 1994 to *Journal of the Acoustical Society of America.*

The research on numerical solutions of the KZK equation concluded with calculations for the propagation of a noise burst radiated from a circular piston source. No calculations have been reported previously in the literature which take into account the combined effects of diffraction, absorption and nonlinearity on the propagation of noise. To construct the noise burst at the source we followed the method employed by Webster and Blackstock.[11] We begin with a frequency spectrum which has constant magnitude in the band $0.5 \leq \omega/\omega_0 \leq 1.5$ and vanishes outside that band, where ω_0 is the center frequency of the band. A pseudorandom waveform was created by dividing the nonzero portion of the spectrum into 56 equally spaced frequency components ω_n, assigning each component a random phase ϕ_n with uniform probability density in the range $-\pi \leq \phi_n \leq \pi$, summing the components together, and normalizing the result by a convenient amplitude factor. A time limited noise burst was created by

multiplying the resulting waveform by a suitable pulse envelope function, to obtain the source waveform at $\sigma = 0$ in Fig. 4. The dimensionless parameter $\sigma = z/z_0$ measures distance z along the axis of the beam in terms of the Rayleigh distance z_0 at the center frequency ω_0. The corresponding spectrum of the source waveform in Fig. 4 is normalized by its peak value, and it is expressed in decibels.

The time waveforms and frequency spectra in Fig. 4 depict the axial propagation of the noise burst. At $\sigma = 0.2$ the waveform appears to have slightly less high frequency content than at the source. Inspection of the corresponding spectrum reveals a dip in the vicinity of $\omega/\omega_0 \simeq 1.26$, in agreement with the prediction by linear theory for the last axial null at that frequency. The algorithm thus accounts properly for the effect of diffraction on the random waveform. Maximum spectral broadening due to harmonic generation and shock formation, including the generation of low frequency components below $\omega/\omega_0 = 0.5$, is attained in the vicinity of $\sigma = 1$. Beyond $\sigma = 1$ the effect of attenuation exceeds that of nonlinearity, and the spectrum is gradually low-pass filtered. The filtering process, which leads to an increase in the relative amplitudes of the nonlinearly generated low frequency components, is demonstrated in the continuation of the calculations in Fig. 5. Because of the irregular amplitude of the source waveform, there is no clearly indentifiable far field waveform which corresponds to self-demodulation. Instead, the waveforms evolve continuously as more and more high frequency components are stripped away by absorption.

Finally, it was noted that Lee's numerical algorithm can be modified to include the effects of relaxation. An augmented Burgers equation, which is coupled with auxiliary relaxation equations, has been developed by Pierce[12] for a thermoviscous fluid with an arbitrary numbers of relaxation processes. The KZK equation can be augmented in a similar way. In our numerical model, however, physical phenomena are decoupled over each propagation step,[9, 10] and we therefore require only the relaxation equation for a small-signal plane wave. It is assumed that the various relaxation processes are independent, and that the νth process is characterized by a relaxation time t_ν and high-frequency propagation speed increment $(\Delta c)_\nu$.[12] Relaxation is included by solving over each step $\Delta\sigma$, in addition to equations which account for diffraction, absorption, and nonlinearity, the following equation:

$$\left(1 + \theta_\nu \frac{\partial}{\partial \tau}\right) \frac{\partial P}{\partial \sigma} = C_\nu \frac{\partial^2 P}{\partial \tau^2}, \tag{21}$$

where θ_ν and C_ν are dimensionless constants that characterize the νth process, P is dimensionless pressure, and τ dimensionless retarded time. All operations are performed in the time domain.

Relaxation effects were recently introduced in Lee's code by R. O. Cleveland (Ph.D. student in Mechanical Engineering), who is investigating the propagation of sonic booms under the supervision of Professor D. T. Blackstock (work supported by NASA). Calculations based on the modified algorithm were compared with an analytic stationary wave solution derived by Polyakova, Soluyan, and Khokhlov[13]

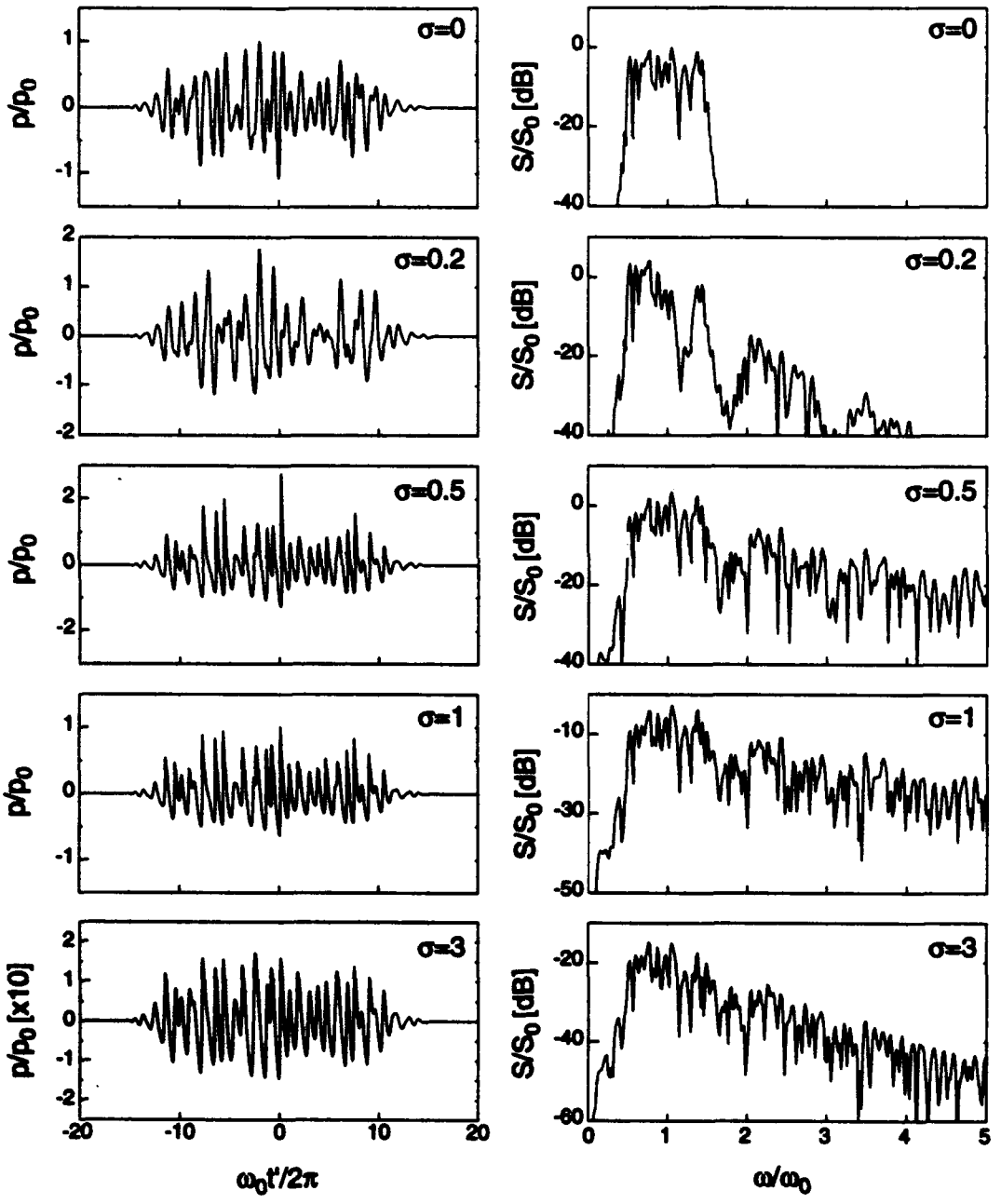

Figure 4: Propagation of a finite amplitude noise burst along the axis of a circular piston radiator.

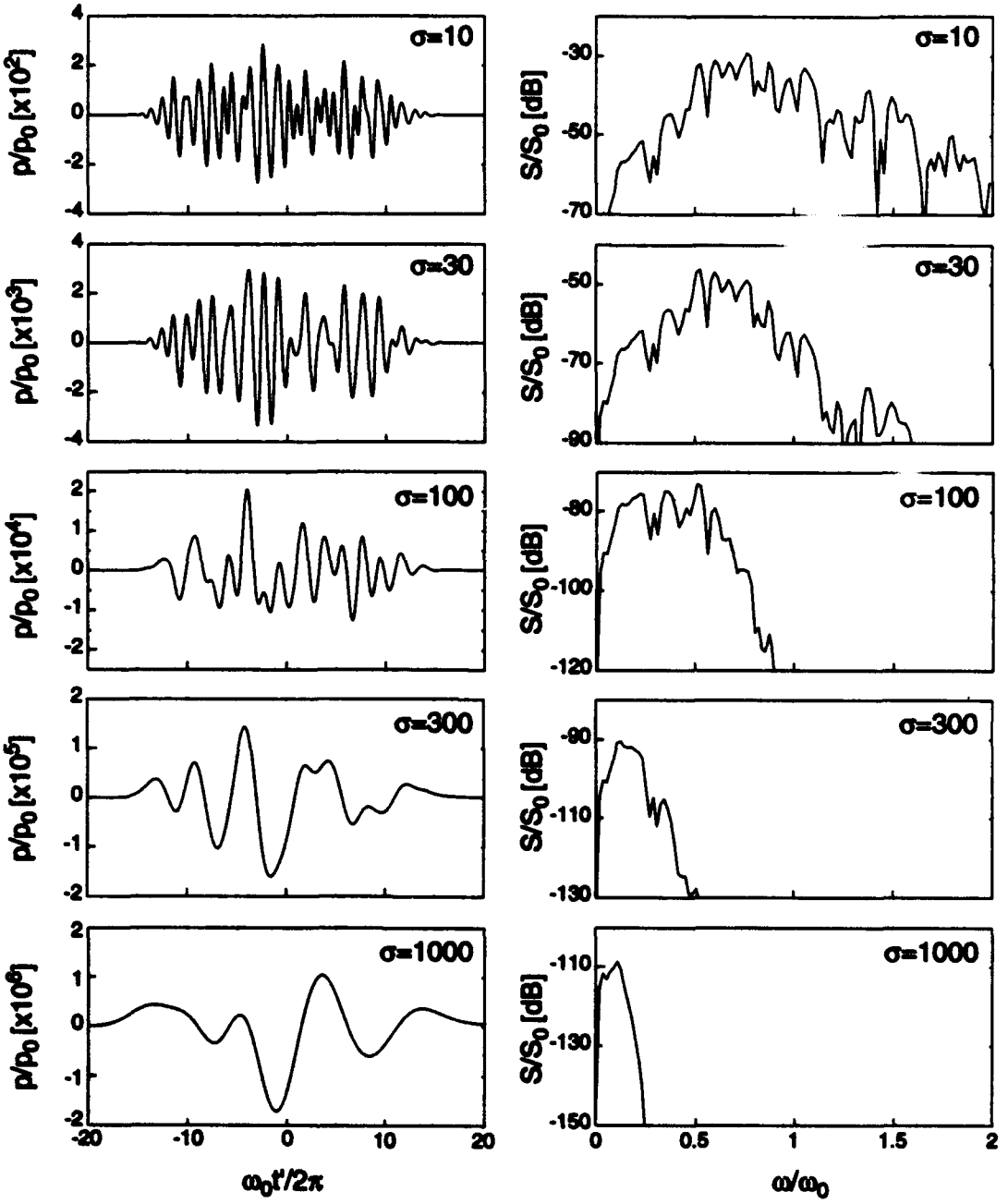

Figure 5: Continuation of Fig. 4.

for the propagation of a step shock in a monorelaxing fluid, and excellent agreement was obtained.[14]

B. Focused Finite Amplitude Sound Beams

The measurements reported below were obtained by M. A. Averkiou, who completed his Ph.D. in Mechanical Engineering for this work in May 1994.[15] His results will be reported in an article that is nearly ready for submission to *Journal of the Acoustical Society of America*. Averkiou is currently employed by Applied Physics Laboratory at the University of Washington.

The purpose of this investigation is to present detailed measurements of harmonic generation in the field of a focused piston source that radiates in water at finite amplitude. The measurements are compared with numerical solutions of the KZK equation. Our work is therefore very similar to that reported previously by Baker.[16] One of our contributions is improvement of the dynamic range and spatial resolution in measurements of the harmonic field structure. These improvements permit comparison with theory to be made with greater precision. Second, measured beam patterns are shown at more locations than have been reported previously in the literature.

Measured (solid lines) and predicted (dashed lines) beam patterns for the first four harmonic components are presented in Fig. 6. A circular source with radius 19 mm and focal length 159 mm was used, which radiated in water at 2.25 MHz. The theoretical predictions are based on numerical solutions of the KZK equation. The equation is solved numerically with the version of the spectral code described by Naze Tjøtta et al.[17] Excellent agreement is obtained between theory and experiment. In particular, the sidelobe structure of all four harmonic components is predicted very accurately in the focal plane, particularly the "fingers" (i.e., additional sidelobes[18, 19]) in the second and higher harmonic beam patterns. Note also the inward shift of the sidelobes in the second and higher harmonic beam patterns, relative to the sidelobe locations in the primary wave beam pattern. Detailed measurement of this effect, and comparison with theory, is presented here for the first time. These phenomena were observed in a numerical investigation of focused beams supported earlier by ONR.[20]

C. Reflection of a Spherical Wave from a Parabolic Mirror

The reflection of a spherical wave from a parabolic mirror is a problem encountered in the analysis of electromagnetic antennas. The incident wave is radiated from the focus of the parabola, and ray theory predicts a collimated, planar reflected wave (see Fig. 7). In reality, diffraction produces a complicated nearfield structure, and the amplitude of the wave in the farfield decreases inversely with distance. Although considerable attention has been devoted to this problem, it appears that all reported

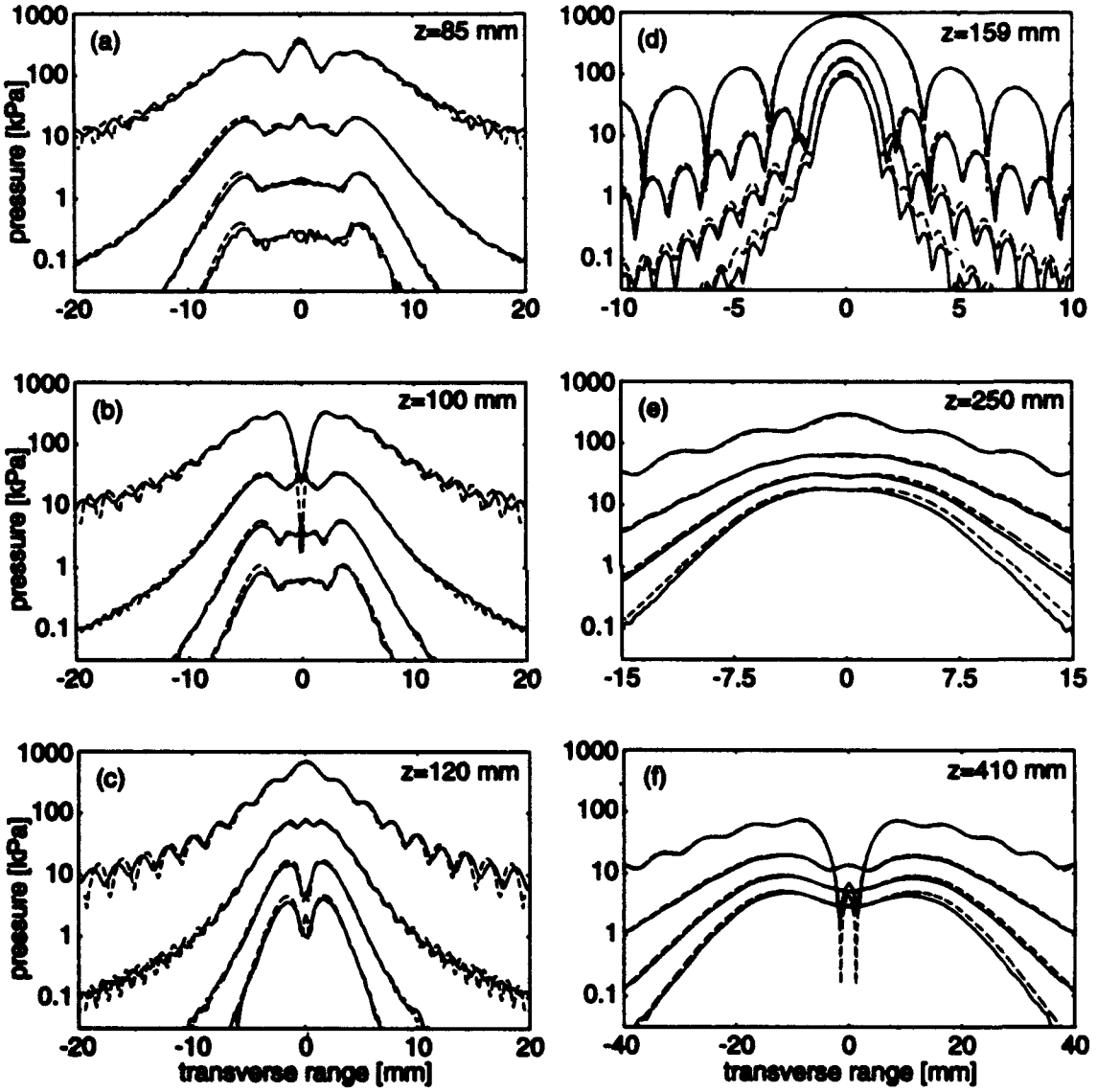

Figure 6: Comparison of theory (dashed lines) and experiment (solid lines) for the first four harmonic beam patterns in a focused sound beam radiated from a circular source.

analyses have been performed in the frequency domain. However, recent interest in the design of ultra-wideband antennas (see, for example, Ref. 21) motivates the derivation of a time domain solution.

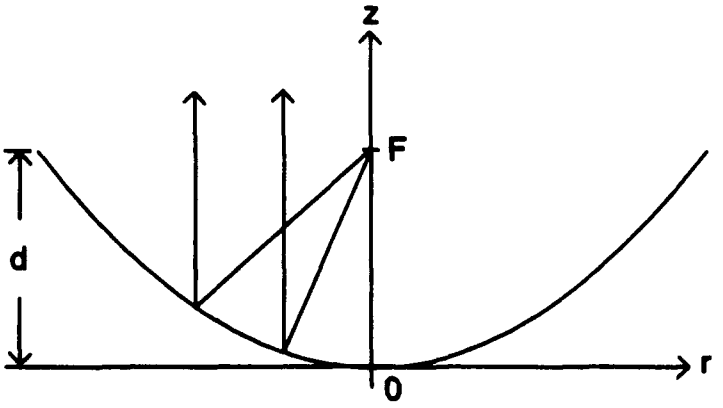

Figure 7: Geometry of parabolic reflector.

The following transient axial solution was derived for the reflection of an acoustic spherical wave from a rigid, parabolic mirror. Our solution complements the experimental work performed recently by D. M. Hester[22] and currently by L. J. Gelin under the supervision of Professor Blackstock. The incident spherical wave p_i radiated from the focus F is assumed to have the form $p_i/p_0 = (F/R)f[t-(R-F)/c_0]$, where p_0 is the pressure of the incident wave at $(r,z) = (0,0)$, $f(t)$ is an arbitrary function of time, R is distance from the focus, and c_0 is the sound speed. Following techniques developed earlier for analysis of reflection from an ellipsoidal mirror,[23] we derived the following solution for the axial pressure in the reflected field:

$$\frac{p_r}{p_0} = f\left(t-\frac{z}{c_0}\right) - h_e(z)f(t-t_e) - \frac{c_0}{F}\int_{z/c_0}^{t_e} h_w(z,t')f(t-t')\,dt', \qquad (22)$$

where t_e is related to the time a signal takes to propagate from the edge of the mirror to the axial observation point, and h_e is the amplitude of the "edge wave." The first term is referred to as the "center wave," and the third term is referred to as the "wake." Simple analytic expressions have been obtained for the impulse response functions $h_e(z)$ and $h_w(z,t)$. For $z > F$ the edge wave amplitude approaches the asymptotic value $h_e \simeq (1+d/F)^{-1}$, where d is the depth of the mirror. In the farfield, Eq. (22) reduces to

$$\frac{p_r}{p_0} \sim \frac{2F^2}{c_0 z}\ln\left(1+\frac{d}{F}\right) f'\left(t-\frac{z}{c_0}\right), \qquad z\to\infty, \qquad (23)$$

where $f'(t) = df/dt$. The derivative of the source waveform is thus obtained in the farfield.

In Fig. 8 we show calculations based on Eq. (22) for the axial reflected field due to a one-cycle sinusoid incident on the mirror. The ratio of mirror depth to focal length was selected to be $d/F = 1.13$, the same as in the experiments performed by Hester[22] and Gelin. The dimensionless pulse duration is $c_0T/F = 0.1$, which is also consistent with experiment and satisfies the assumption in the derivation of Eq. (22) that the wavelength is small in comparison with the dimensions of the reflector. At $z/F = 10$ the center wave (on the left in Fig. 8) and edge wave (on the right) are clearly resolved, and the effect of the wake is insignificant. At $z/F = 20$ the amplitude of the edge wave has increased slightly, and the effect of the wake is becoming noticeable. As the center and edge waves overlap, the wake plays an increasingly greater role. In the farfield, at $z/F = 1000$, the derivative of the incident waveform is obtained, and the pulse amplitude decreases in proportion to distance, as predicted by Eq. (23).

III. Fluid-Solid Interface Effects

This investigation is being performed by B. J. Landsberger, who has been funded through AASERT since fall 1993. Landsberger's AASERT funding is separate from the AASERT funding for Meegan (whose work is discussed in Sec. ID). Meegan's funding is administered through the "parent" ONR Grant N00014-89-J-1003, whereas ONR Grant N00014-93-1-1135 was created specifically to administer Landsberger's funding.

Both experiment and theory were proposed for an investigation of diffracting sound beams that are scattered in liquids following interaction with elastic half spaces and plates. These are classic problems that are studied in connection with ultrasonic nondestructive evaluation, and they have received considerable attention in the literature. However, the following observations can be made about the current state of research on these problems: (1) there are scarcely any high precision, quantitative field measurements of the scattered (i.e., reflected and transmitted) sound beams, (2) most theories are developed for either two-dimensional or Gaussian sound beams, whereas three-dimensional beams radiated by uniform sources are used in practice, and (3) effects of nonlinearity are virtually unexplored. The proposed research is intended to address each of these points through both experiments and analysis.

Despite the numbers of experiments reported on the interactions of sound beams with elastic half spaces and plates, most published data provide only qualitative descriptions of the related effects due to diffraction and mode generation. Specifically, the primary method of data acquisition has been Schlieren visualization. Schlieren images provide dramatic confirmation of physical phenomena such as beam displacements for incidence near Rayleigh and Lamb angles, and of different modes of leaky wave radiation from the solid into the surrounding fluid. However, Schlieren images do not provide the precision that is needed for quantitative comparisons with theory.

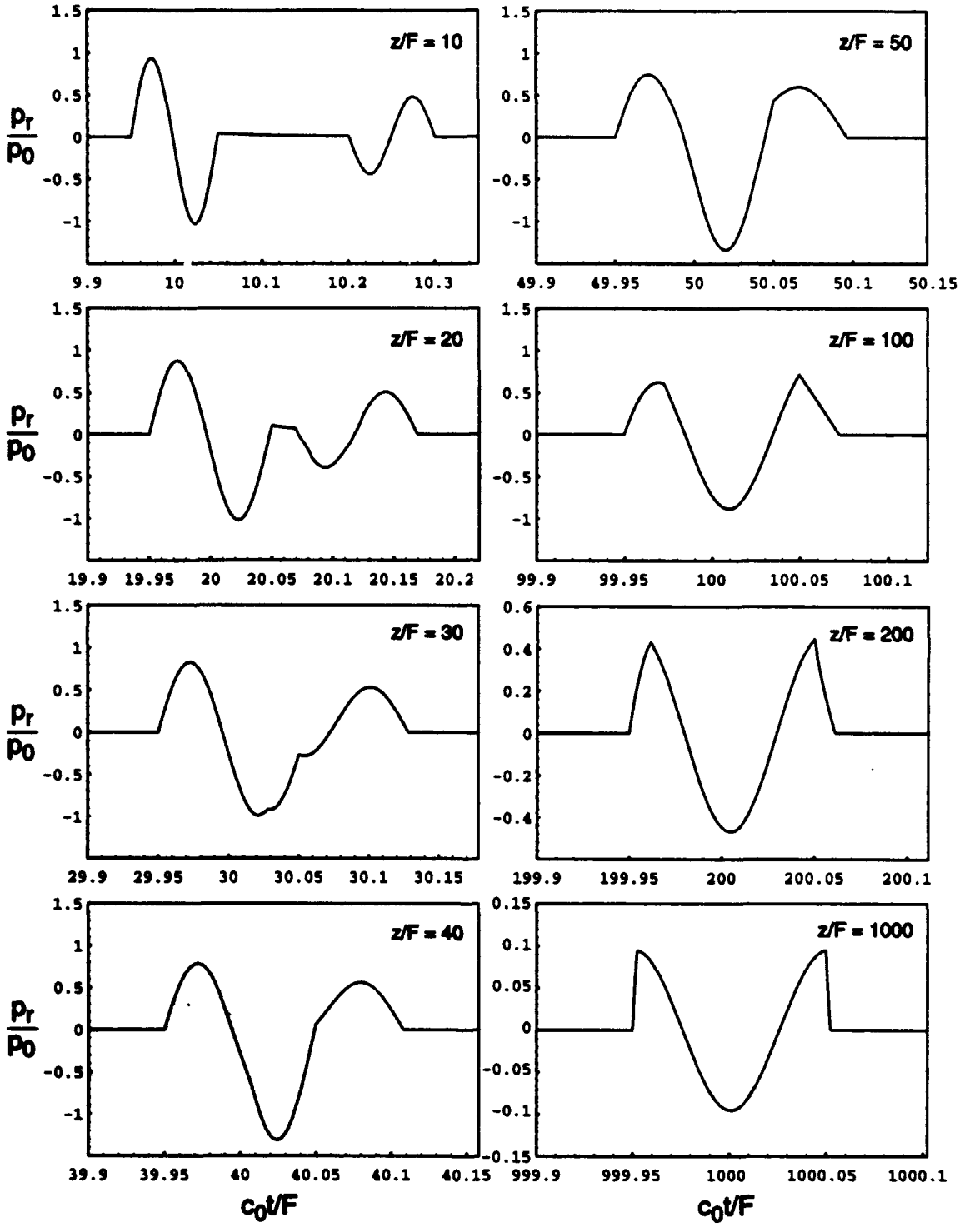

Figure 8: Reflected sinusoidal pulse along the axis of a parabolic mirror.

This fact has been noted in recent years by others,[24] and it appears to influence the directions of current theoretical investigations. For example, theories that account for diffraction in three dimensions (3-D) are normally restricted to Gaussian beams,[25] and theories for sound beams radiated by uniform pistons normally account for only 2-D diffraction.[24, 26] Even within the past two years,[27] measurements obtained with a (3-D) circular piston source were compared with theory based on a 2-D Gaussian source, and the results are said to be in quantitative agreement. More recently, a rectangular Gaussian source with large aspect ratio (to approximate a 2-D Gaussian source) was used to generate reflected fields that could be compared more consistently with 2-D Gaussian beam theory.[28] However, noticeably absent from the literature are comparisons of theory for 3-D circular pistons with measurements obtained with conventional circular ultrasonic sources, even in the small signal limit where nonlinear effects can be ignored.

The first goal was therefore to develop a computer program which calculates the reflection of an arbitrary 3-D sound beam from a liquid-solid half space. This is a necessary first step toward comparison with measurements to be made using standard circular piston sources in the Mechanical Engineering ultrasonics tank facility. The code is based on numerical solution via 2-D spatial FFT of the following standard reflection integral:

$$P_r(x,y,z) = \frac{1}{4\pi^2}\int\!\!\int_{-\infty}^{\infty} \tilde{P}_i(k_x,k_y,z_i)R(k_x,k_y)e^{i(k_x x+k_y y+k_z z)}\,dk_x dk_y\,, \qquad (24)$$

where P_r is the spatial component of the reflected pressure field, $\tilde{P}_i$ the FFT of the incident beam in the plane of the interface $z = z_i$, k_x and k_y are wavenumbers in the (x,y) plane, $k_z = (\omega^2/c_0^2 - k_x^2 - k_y^2)^{1/2}$ is the wavenumber perpendicular to the interface, and R is the plane wave reflection coefficient. We note that focusing is easily taken into account with the computer code.

Somewhat surprisingly, we have not found published 3-D solutions of Eq. (24) for the practical case of reflection produced by incident radiation from a circular piston source. We show such calculations in Fig. 9. Figure 9(a) shows the calculated pressure distribution of a 1 MHz beam radiated from a one-inch diameter circular piston in water, incident on a planar steel interface. The transducer is 10 cm from the interface, and the axis of the incident beam forms an angle of 31° (the Rayleigh angle) with the interface. The coordinate axes along the perimeters of the plots mark position on the interface in centimeters, and the vertical axes denote dimensionless pressure amplitudes. In Fig. 9(b) is shown the calculated pressure distribution in the reflected beam right at the interface. Note the complicated sidelobe structure, in both the incident and reflected fields, which characterizes sound fields radiated from circular pistons. The bimodal distribution in the reflected field is due to the well known interference between the specularly reflected wave and radiation from the interface wave. The peak directly in the center of Fig. 9(b) is due mainly to the specular reflection, as seen by comparison with Fig. 9(a).

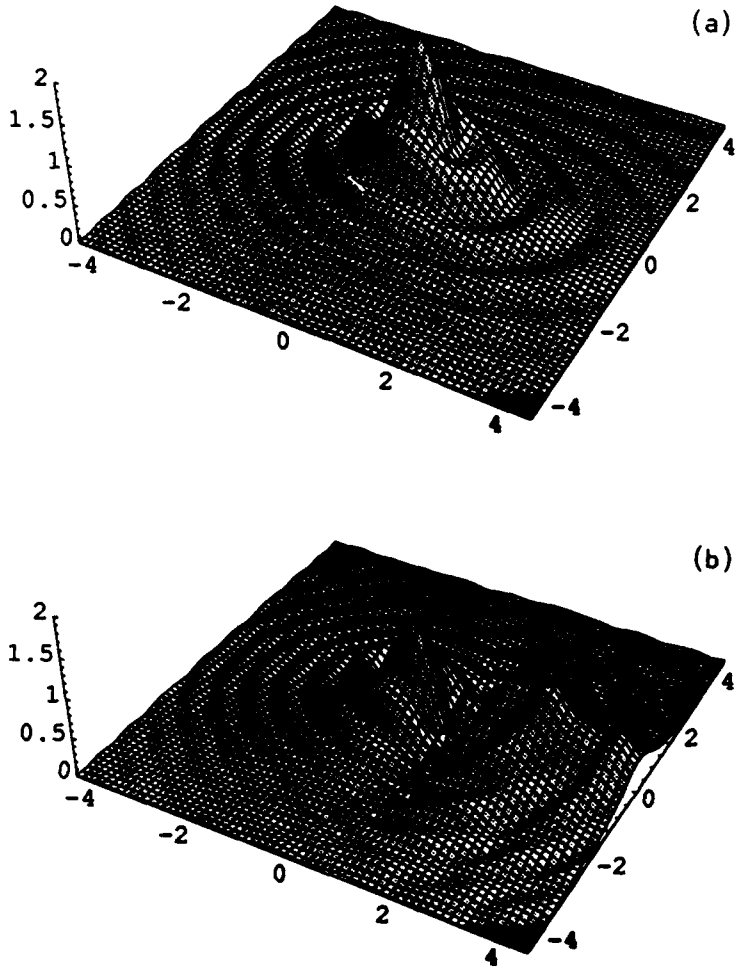

Figure 9: Surface plots of (a) incident and (b) reflected pressure distributions at the interface formed by water and steel.

In Fig. 10(a) are shown the superposed incident and reflected pressure distributions along the lines of symmetry in Fig. 9(a) and 9(b). The reflected field distribution 10 cm away from the interface is shown in Fig. 10(b). The field structure and overall amplitude has been altered by diffraction. For comparison, the curves in Fig. 10(c) and 10(d) are calculated for 2-D radiation from a Gaussian source (which is commonly studied in the literature), but otherwise the parameters are the same as in the left column. Although the classical bimodal pressure distribution is clearly revealed by the 2-D Gaussian beam theory, the fine structure seen in the piston field is absent, and comparison of the beam patterns at $z = 0$ cm and $z = 10$ cm shows only minor diffraction effects due to propagation over that distance (in comparison to the piston radiation).

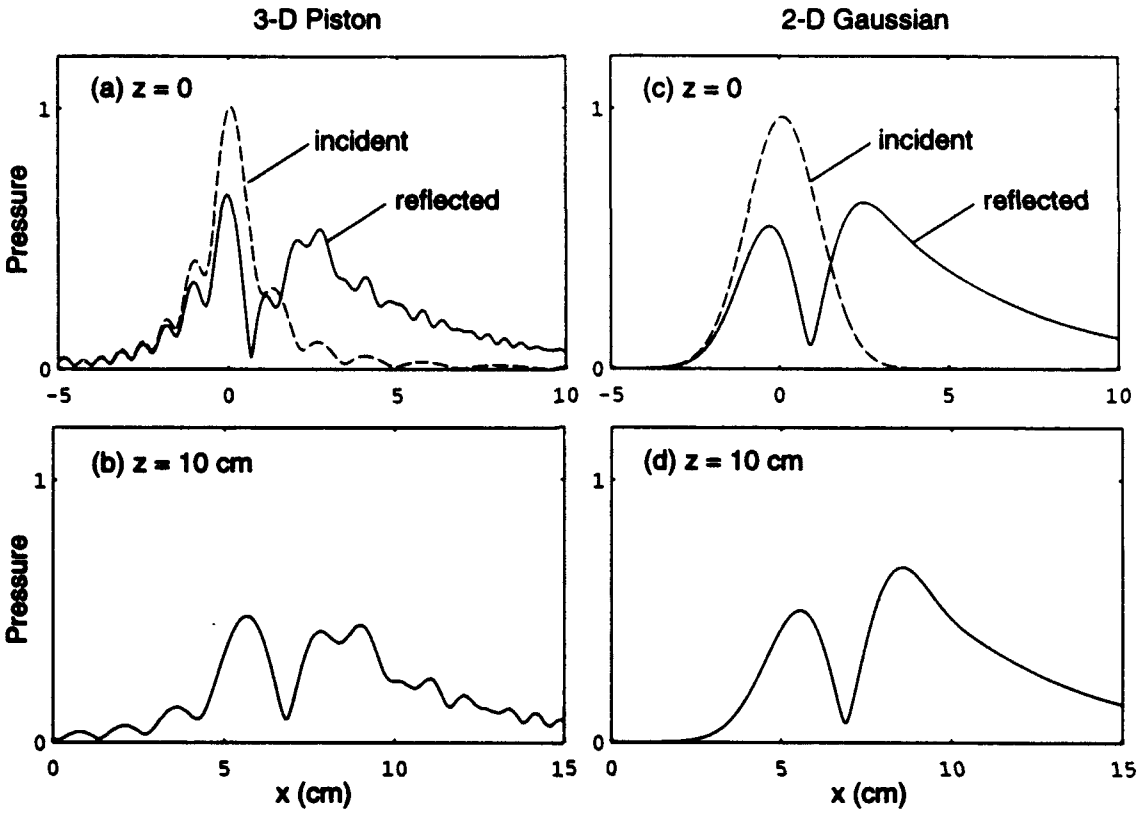

Figure 10: Incident (dashed lines) and reflected (solid lines) beam patterns due to circular piston radiation (a) at the water-steel interface, and (b) 10 cm away from the interface. Comparable results based on 2-D Gaussian beam theory: (c) and (d).

Landsberger is currently following two paths. One is the beginning of experiments with elastic half-spaces and plates, the results from which will be compared with the small signal results predicted by Eq. (24). The ultimate objective, however, is to determine whether measurements of the third order elastic constants can be made by monitoring the properties of harmonic generation in the reflected beam (or perhaps the transmitted beam in the case of plates). To this end, Landsberger has completed a rederivation of results obtained by Cotaras[29] for the reflection and transmission of finite amplitude sound at a fluid-fluid interface. This work will next be generalized to reflection and transmission at a fluid-solid interface.

BIBLIOGRAPHY

[1] E. A. Zabolotskaya, "Nonlinear propagation of plane and circular Rayleigh waves in isotropic solids," *J. Acoust. Soc. Am.* **91**, 2569–2575 (1992).

[2] M. F. Hamilton, Yu. A. Il'insky, and E. A. Zabolotskaya, "Nonlinearity in Rayleigh waves," submitted to *J. Acoust. Soc. Am.* in October 1993.

[3] M. F. Hamilton, Yu. A. Il'insky, and E. A. Zabolotskaya, "Evolution equations for nonlinear Rayleigh waves," submitted to *J. Acoust. Soc. Am.* in February 1994.

[4] D. T. Blackstock, "Thermoviscous attenuation of plane, periodic, finite-amplitude sound waves," *J. Acoust. Soc. Am.* **36**, 534–542 (1964).

[5] N. S. Bakhvalov, Ya. M. Zhileikin, and E. A. Zabolotskaya, *Nonlinear Theory of Sound Beams* (American Institute of Physics, New York, 1987).

[6] D. J. Shull, M. F. Hamilton, Yu. A. Il'insky, and E. A. Zabolotskaya, "Harmonic generation in plane and cylindrical nonlinear Rayleigh waves," *J. Acoust. Soc. Am.* **94**, 418–427 (1993).

[7] D. J. Shull, E. E. Kim, M. F. Hamilton, and E. A. Zabolotskaya, "Diffraction effects in nonlinear Rayleigh wave beams," submitted to *J. Acoust. Soc. Am.* in December 1993.

[8] D. F. Parker, "Waveform evolution for nonlinear surface acosutic waves," *Int. J. Eng. Sci.* **26**, 113–118 (1985).

[9] Y.-S. Lee, "Numerical solution of the KZK equation for pulsed finite amplitude sound beams in thermoviscous fluids," Ph.D. Dissertation, The University of Texas at Austin (December 1993).

[10] Y.-S. Lee and M. F. Hamilton, "Time domain modeling of pulsed finite amplitude sound beams," submitted to *J. Acoust. Soc. Am.* in March 1994.

[11] D. A. Webster and D. T. Blackstock, "Collinear interaction of noise with a finite-amplitude tone," *J. Acoust. Soc. Am.* **63**, 687-693 (1978).

[12] A. D. Pierce, *Acoustics—An Introduction to Its Physical Principles and Applications* (Acoustical Society of America, New York, 1989), p. 587.

[13] A. L. Polyakova, S. I. Soluyan, and R. V. Khokhlov, "Propagation of finite disturbances in a relaxing medium," *Sov. Phys. Acoust.* **8**, 78-82 (1962).

[14] R. O. Cleveland, M. F. Hamilton, and D. T. Blackstock, "Effect of stratification and geometrical spreading on sonic boom rise time," Proceedings of the NASA High Speed Research Program Sonic Boom Workshop, NASA Langley Research Center, Virginia, June 1–3 (1994).

[15] M. A. Averkiou, "Experimental investigation of propagation and reflection phenomena in finite amplitude sound beams," Ph.D. Dissertation, The University of Texas at Austin (May 1994).

[16] A. C. Baker, "Nonlinear pressure fields due to focused circular apertures," *J. Acoust. Soc. Am.* **91**, 713–717 (1992).

[17] J. Naze Tjøtta, S. Tjøtta, and E. H. Vefring, "Effects of focusing on the nonlinear interaction between two collinear finite amplitude sound beams," *J. Acoust. Soc. Am.* **89**, 1017–1027 (1991).

[18] J. Berntsen, J. Naze Tjøtta, and S. Tjøtta, "Nearfield of a large acoustic transducer. Part IV: Second harmonic and sum frequency radiation," *J. Acoust. Soc. Am.* **75**, 1383–1391 (1984).

[19] M. F. Hamilton, J. Naze Tjøtta, and S. Tjøtta, "Nonlinear effects in the farfield of a directive sound source," *J. Acoust. Soc. Am.* **78**, 202–216 (1985).

[20] T. S. Hart and M. F. Hamilton, "Nonlinear effects in focused sound beams," *J. Acoust. Soc. Am.* **84**, 1488–1496 (1988).

[21] H. L. Bertoni, L. Carin, and L. B. Felsen, eds., *Ultra-Wideband, Short-Pulse Electromagnetics* (Plenum, New York, 1993).

[22] D. M. Hester, "N wave field produced by a paraboloidal reflector and application to microphone calibration," M.S. Report, The University of Texas at Austin (May 1992).

[23] M. F. Hamilton, "Transient axial solution for the reflection of a spherical wave from a concave ellipsoidal mirror," *J. Acoust. Soc. Am.* **93**, 1256–1266 (1993).

[24] K. W. Ng, T. D. K. Ngoc, I. Molinero, and M. de Billy, "Measurement of the profile of an ultrasonic beam non-specularly reflected from a solid plate," *Ultrasonics* **26**, 44–46 (1988).

[25] J. D. Harris and J. Pott, "Further studies of the scattering of a Gaussian beam from a fluid-solid interface," *J. Acoust. Soc. Am.* **78**, 1072–1080 (1985).

[26] T. D. K. Ngoc and W. G. Mayer, "Numerical integration method for reflected beam profiles near Rayleigh angle," *J. Acoust. Soc. Am.* **67**, 1149–1152 (1980).

[27] T. E. Matikas, M. Rousseau, and P. Gatignol, "Experimental study of focused ultrasonic beams reflected at a fluid-solid interface in the neighborhood of the Rayleigh angle," *IEEE Trans. Ultrason. Ferr. Freq. Cont.* **39**, 737–744 (1992).

[28] D. E. Chimenti, J.–G. Zhang, S. Zeroug, and L. B. Felsen, "Interaction of acoustic beams with fluid-loaded elastic structures," *J. Acoust. Soc. Am.* **95**, 45–59 (1994).

[29] F. D. Cotaras, "Reflection and refraction of plane acoustic waves of finite amplitude at a plane fluid-fluid interface," Ph.D. dissertation, The University of Texas at Austin (1989).